



ISSN: 0067-2904

## Effect of a rising time of the lightning impulse on streamer discharge behavior

Noor A. Ahmed, Thamir H. Khalaf

Physics Department, College of Science, University of Baghdad, Baghdad, Iraq;

Received: 5/5/2024

Accepted: 27/10/2024

Published: 30/11/2025

### Abstract

A numerical simulation of the streamer discharge was constructed to study the streamer origination (initiation) of the streamer discharge formation and development between two electrodes, one of which is a needle and the other a sphere electrode in transformer oil, with focusing on the effect of the rising time of lightning impulse voltage between the two electrodes. The model includes electron, positive, and negative ion continuity equations and Poisson's equation to simulate this streamer discharge behavior. The growth and development of the streamer discharge are examined by changing the rising time it takes for the voltage to increase using the applied impulse voltage parameters. Additionally, this model investigates different characteristics of the streamer discharge, such as the distribution of the electric field, time initiation of the streamer discharge at the electrode (needle), streamer discharge velocity, streamer diameter, and minimum breakdown voltage for each case of the rising time. The results showed that increasing the rising time (25-100ns), increasing the time initiation (6-19ns), and decreasing the streamer's electric field before it. ( $4.75 \times 10^8 - 4.38 \times 10^8 \text{ v/m}$ ), decreases the streamer velocity (2.353-1.421km/s), the streamer diameter (0.175-0.167mm), and increases the voltage breakdown (79-100kv). The simulation was done in a virtual cell filled with transformer oil with a gap of 1mm between the two electrodes.

**Keywords:** Streamer discharge, Cosmol Multiphysics, Transformer oil, Rising time, streamer velocity.

### تأثير زمن صعود نبضة البرق على سلوك تفريغ التدفق

نور علاء احمد , خلف ثامر حميد

قسم الفيزياء , كلية العلوم , جامعة بغداد , بغداد , العراق

### الخلاصة

تم بناء محاكاة عددية لتفريغ التدفق لدراسة نشوء (بدء) تفريغ التدفق وتطوره بين قطبين أحدهما أبرة والقطب الآخر كرة في زيت المحولات، مع التركيز على تأثير زمن صعود نبضة الفولتية المسلطة بين القطبين. يتضمن نموذج المحاكاة معادلات الاستمرارية للإلكترونات والأيونات الموجبة والسالبة وكذلك معادلة بواسون لدراسة سلوك تفريغ التدفق، حيث يتم تتبع نمو وتطور تفريغ التدفق مع تغيير زمن الصعود الذي يستغرقه زيادة الجهد باستخدام معلمات الجهد النبضي المطبقة. بالإضافة إلى ذلك، يبحث هذا النموذج في

سمات مختلفة لتفريغ التدفق، مثل توزيع المجال الكهربائي، زمن نشوء تفريغ التدفق عند القطب (الابرة) وسرعة تفريغ التدفق وكذلك قطر التدفق، والحد الأدنى من جهد الانهيار لكل حالة من حالات زمن الصعود. أظهرت النتائج أنه مع زيادة زمن الصعود (25-100 نانو ثانية) يزداد زمن النشوء (6-19 نانوثانية) وينخفض المجال الكهربائي في مقدمة التدفق ( $4.75 \times 10^8$  -  $4.38 \times 10^8$  فولت /متر) وتنخفض سرعة تفريغ التدفق (2.353 - 1.421 كيلومتر/ثانية) ويقل قطر التدفق (0.167 - 0.175 ملم) وتزداد فولتية الانهيار (79 - 100 كيلو فولت). جرت المحاكاة في خلية افتراضية مملوءة بزيوت المحولات يفصل القطبين 1 ملليمتر.

**الكلمات المفتاحية:** تفريغ التدفق، برنامج الكومسول، زيت المحولات، زمن الصعود، سرعة تفريغ التدفق.

## 1. Introduction

Because of their favorable electrical properties, transformer oil and other dielectric fluids are used in high-voltage electrical gear and pulsed power systems. In powerful electric fields and throughout possible breakdown processes, these fluids display intriguing electrical properties that make them extremely valuable in real-world applications [1]. Liquid insulators are frequently chosen over solid or gaseous dielectric materials because of their better performance in various applications [2]. Depending on the strength of the electric field, transformer oil produces streamers as a result of the hydrocarbon molecules being chemically ionized [3-4]. In recent years, much theoretical and experimental work has been done to study the properties of velocity, field electrical distribution, and streamer morphology of liquid dielectrics [5-6]. One of the numerous factors that might influence how streamers behave when released into transformer oil is the lengthening lightning impulse. The rising time is the period needed for a lightning impulse's voltage to peak. The impact of rising time on streamer behaviors, insulation deterioration, and potential transformer damage should be taken into account while building and operating electrical transformers since streamers can produce partial discharge. Higher rates of voltage change and strong electrical fields in the transformer's oil could be caused by lightning impulses with shorter rising periods. Thus, this may impact streamers' start, development, and behavior [7]. Equipment failures and large financial losses could be among the worst effects of power transformer insulation losses. As a result, many studies have been conducted to determine the insulation value of transformer oils. Akiyama [8], Lesaint et al. [9], Linhjell et al. [10], and Salazar et al. [11] have examined at various voltage levels, the features of streamers in transformer oil, such as their amplitude, polarity, waveform, length, rising and falling times, and speed. Their research focused on comprehending the impact of clouding and investigating different streamer properties in transformer oil [11]. Jadidian Jouya [12].

The main goals of this research are to evaluate the risk of insulation failures, look at ways to lower the risk of mistakes and create plans to lessen the harm that results. This study provides information concerning the causes of electrical discharge, develops mitigation, and presents prevention techniques for transformer failures. The structure of the paper is as follows: In Section 1, the governing and boundary equations of the electro-thermal hydrodynamic model are explained in detail, and in Section 2 the behavior of streamer discharges is analyzed about the rising time of the lightning impulse.

## 2. MODELING AND SIMULATION

### 2.1 The model's characteristics and description

The complex chemical reaction caused by the electrical field in transformer oil is hard to describe in words alone. A charge source is the result of this ionization reaction.

Understanding and reproducing this phenomenon is challenging due to the oil's complicated chemical composition and the absence of a thorough theory covering the behaviors of liquid dielectrics. [13]. In transformer oil, field ionization during the discharge event is primarily responsible for the generation of negative and positive ions, as well as free electrons. A high electric field raises one electron to the conductivity band of a neutral molecule, resulting in free electrons, negative and positive ions [4]. This process, which helps to better explain how the streamer discharge propagates, is called field ionization [5]. They discovered that the ionizing potentials of the liquid's molecules and density correlated negatively with field ionization in liquids.

The process of molecule ionization caused by an electric field is a basic reason for the formation of streamers in transformer oil, as proven by the work of O'Sullivan et al. [3]. This ionization process turns oil molecules into electrons that move quickly and positive ions that move slowly. When highly mobile electrons leave the ionization zone, leaving behind fewer positive ions, an area of net space charge is formed. This net charge alters the distribution of the electric field inside the oil. Specifically, there is a decrease in the electric field toward the needle electrode and a rise in the electric field toward the ionized area in the oil. This changed electric field distribution causes ionization to occur at points further away from the positive electrode, which in turn causes more changes to the electric field distribution [26,27].

## 2.2 Governing Equations

To understand the mechanism of streamer discharge initiation and development in a dielectric medium, hydrodynamic equations must be studied in the presence of liquids.

Together with the Poisson equation characterizing the electric fields, these equations represent the equations guiding the conservation of three charges for electrons ( $\rho_e$ ), positive ions ( $\rho_p$ ), and negative ions ( $\rho_n$ ). The following equations, derived from these considerations, describe the phenomenon [3]:

$$\nabla \cdot (\epsilon_1 \vec{E}) = \rho_p + \rho_n + \rho_e \quad (1)$$

$$\frac{\partial \rho_p}{\partial t} + \nabla \cdot (\rho_p \mu_p \vec{E}) - \frac{\rho_p \rho_e R_{pe}}{e} - \frac{\rho_p \rho_n R_{pn}}{e} = G_I(|\vec{E}|) \quad (2)$$

$$\frac{\partial \rho_e}{\partial t} - \nabla \cdot (\rho_e \mu_e \vec{E}) + \frac{\rho_p \rho_e R_{pe}}{e} - \frac{\rho_e}{\tau_a} = -G_I(|\vec{E}|) \quad (3)$$

$$\frac{\partial \rho_n}{\partial t} - \nabla \cdot (\rho_n \mu_n \vec{E}) + \frac{\rho_p \rho_n R_{pn}}{e} - \frac{\rho_e}{\tau_a} = 0 \quad (4)$$

In these equations,  $\epsilon$  represents the relative permittivity of the dielectric material (with a specific value of 2.2 for the transformer oil). The dielectric fluid's ionization sources term, which responds to the electric field, is indicated by  $G_I(|\vec{E}|)$ . The electric charge is expressed by  $q$ , and the electric field is expressed by  $\vec{E}$ . For ions-electrons and ions-ions, the recombination rate constants in the dielectric fluid are  $R_{pe}$  and  $R_{pn}$ , respectively. The attachment time is represented by  $\tau_a$ , whilst the concentrations of electrons, positive ions, and negative ions are represented by  $\rho_e$ ,  $\rho_p$ , and  $\rho_n$ , respectively. The mobility of electrons, negative ions, and positive ions is represented by the symbols  $\mu_e$ ,  $\mu_n$ , and  $\mu_p$ , respectively. These annotations and parameters are taken from the works [3,4,6]

$$G_F(|\vec{E}|) = \frac{q^2 n_0 \alpha |\vec{E}|}{h} \exp\left(-\frac{\pi^2 m^* \alpha \Delta^2}{q h^2 |\vec{E}|}\right) \quad (5)$$

Where:  $n_0$  is the concentration of ionizable transformer oil,  $\Delta$  is the molecule's ionization energy,  $h$  is Planck constant,  $m^*$  is the electron effective mass,  $a$  is the distance between molecules, and  $q$  is the electron charge. For this investigation, the primary physical parameters necessary for the simulation model were obtained from previously published literature [3,16,17,18], as presented in Table (1).

**Table 1:** The most important variables employed in the model.

Symbol	Parameter	value
$\Delta$	Electrical potential ionization	8.25eV
$n_0$	Ionizable species density	$1 \times 10^{23} m^{-3}$
$\alpha$	Distance between molecule	$3 \times 10^{-10} m$
$e$	Electron charge	$-1.6 \times 10^{-19} C$
$m^*$	The electron-effective mass	$9.1 \times 10^{-32} kg$
$R_{pe}, R_{pn}$	Ratios of electron-ion and ion-ion recombination	$1.64 \times 10^{-17} m^3/s$
$\mu_p \mu_n$	Positive and negative ions' mobility	$1 \times 10^{-9} m^2/vs$
$\mu_e$	Electron mobility	$1 \times 10^{-4} m^2/vs$
$\tau_a$	Constant electron attachment time	$200 \times 10^{-9} s$
$\epsilon_0$	Permittivity in vacuum	$8.85 \times 10^{-12} F/m$
$\epsilon_1$	Oil permittivity	$2.2 \epsilon_0 F/m$
$h$	Planck constant	$6.6310^{-34} m^2 kg/s$

### 2.3. Computation Domain

As illustrated in Figure 1a, a cylindrical virtual cell containing transformer oil and a needle-sphere electrode configuration meeting the specifications outlined in the IEC 60897 Standard [19] was hypothesized to solve the model. A side of the cell's cross-section represents the domain of the solution since the model, which was solved in two dimensions, is symmetric about  $z$  (Figure 1b). The solution was obtained based on the finite element technique, which required a discretization for the domain to a small finite element as a mesh, as shown in Figure 1c. The mesh was designed to have a high density of elements around the electrodes and along the symmetry line where the parameters varied strongly.

The spherical electrode has a curvature radius of 6.35 mm, and the needle electrode at the tip has a curvature radius of 40  $\mu m$ . The distance between the electrodes was set at 1 mm. The overall dimensions of the domain are  $r \times z = 22 \text{ mm} \times 12.5 \text{ mm}$ . The design chosen and drawn using the AutoCAD program can be imported into the COMSOL Multiphysics program to facilitate the process. The domain is composed of a needle representing the anode and a sphere electrode representing the cathode.

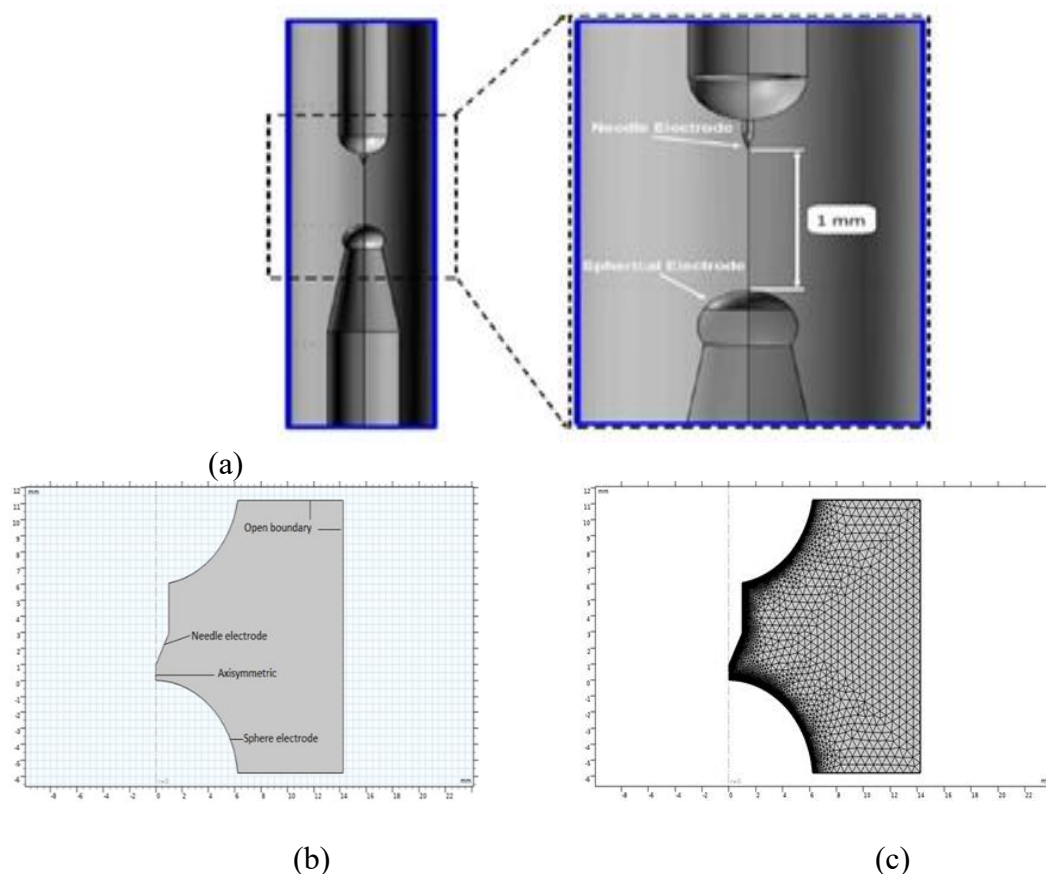


**Figure 1:** The geometry of the needle-sphere electrode, following the specifications outlined in the IEC 60897 standard: (a) the complete geometry, (b) the solution domain, and (c) the discretization mesh.

#### 2.4. Boundary and numerical condition

The boundary and spatial conditions for the equations must be established after the model design is ready to be solved. The insulated walls were subject to a zero-charge boundary condition in this situation. In the electrostatic process, Equation 1 defines the Poisson equation.  $V=0$ , or the ground potential, is the voltage assigned to the sphere-type electrode, and  $V=V_i$ ,  $V_i$  being the needle electrode-specific potential, is the potential applied to the needle-type electrode. It should be mentioned that the electric field lines are unaffected by the insulating walls. According to IEC 60060-1 [14], a typical voltage connected to a lightning strike can be subtracted from two exponential functions to find the voltage that is applied to the electrode of the needle type:

$$V_i = KV_0 \left( e^{-\frac{t}{\tau_1}} - e^{-\frac{t}{\tau_2}} \right) \quad (6)$$

Where:  $K$  is a non-dimensional compensating factor. Two exponential functions must be subtracted to keep the impulse voltage peak nearly equal to  $V_0$ . The rising time is represented by  $\tau_1$ , while the falling time is represented by  $\tau_2$ . In most circumstances, the greatest value obtained by subtracting the exponential values of the functions is not equal to 1 [20]. Considering the Charge Transport Continuity Equations (2) to (4): At the outer insulating boundaries, the electrode boundary conditions are defined as convective fluxes for all species. Outflow boundary conditions for the sphere-type electrode potential and the needle-type electrode potential apply to the three-carrier continuity equations. The outer boundary does not have any specific flux boundary requirements for these equations. The streamer discharge hydrodynamic model was solved with COMSOL Multiphysics version 6.0. The

"Electrostatic" module was utilized to calculate Poisson's equation (Equation 1), while the "Transport of Diluted Species" module was employed to solve the carrier continuity Equations (2) to (4). Figure 2 illustrates the flowchart depicting the simulation process from start to end, including the acquisition of results.

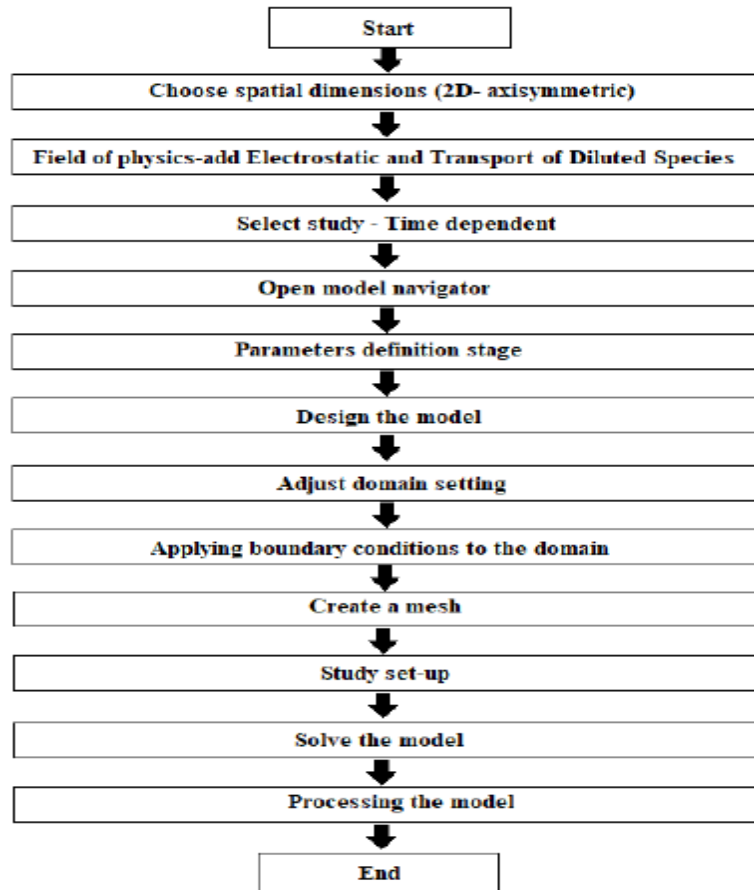


**Figure 2:** Flow chart of the simulation process

### 3. Results and Discussions

Tracking and analyzing the streamer discharge's onset and progression inside the configuration is the aim of the simulation to characterize its dynamics along the electrode distance. The effects of the rising time on the streamers' properties, including their initiation time, velocity, radius, and breakdown voltage, were also investigated. The data presented by Beroual et al. indicated that a high electric field strength of roughly  $2 \times 10^8$  V/m or more is necessary to initiate streamer discharge in transformer oil. Therefore, from its initiation at the needle electrode tip to its breakdown at the sphere electrode, the streamer was represented by the distribution of electric fields between the electrodes.

The processes of streamer discharge initiation, different growth times, and breakdown in transformer oil were examined. The impact of the rising time of the lightning impulse on the behavior of streamer discharge was also investigated.

#### 3.1. Streamer Initiation and Growth

The dynamics of the streamer discharge were studied by tracking the streamer initiation and growth between the two electrodes. This was done by executing the simulation along the

time required for the streamer to bridge the gap between the two electrodes and the occurrence of breakdown. The breakdown occurs at a minimum voltage needed for the streamer to bridge the 1mm gap. To find the minimum breakdown voltage, several simulation tests were executed and determined at 85 kV with a rising time of 50 ns. The streamer spent 356 ns traveling from initiation to breakdown.

As mentioned above, the initiation of the streamer requires a high electric field value equal to or greater than  $2 \times 10^8$  V/m. So, to indicate the initiation and growth of the streamer, the electric field distribution was presented as a surface distribution, as shown in Figure 3, and for more clarity, as a line graph as in Figure 4, at different times from the initiation to the breakdown. The color gradation represented the electric field values from minimum (blue) to maximum (red).

As the streamer discharge moves along the axis of the needle-sphere electrode, the head of the discharge exhibits the highest concentration of electric field, as demonstrated in Figures 3 and 4. These results are in line with previous studies [22, 23]. The strongest electric field constantly travels from the needle to the sphere electrode due to the ionization of the oil molecules and the distortion of the electric field brought on by the space charge. When the streamer discharge enters the electrode gap, this phenomenon which resembles ionizing waves occurs. When the streamer discharge hits the sphere electrode, the breakdown event occurs.

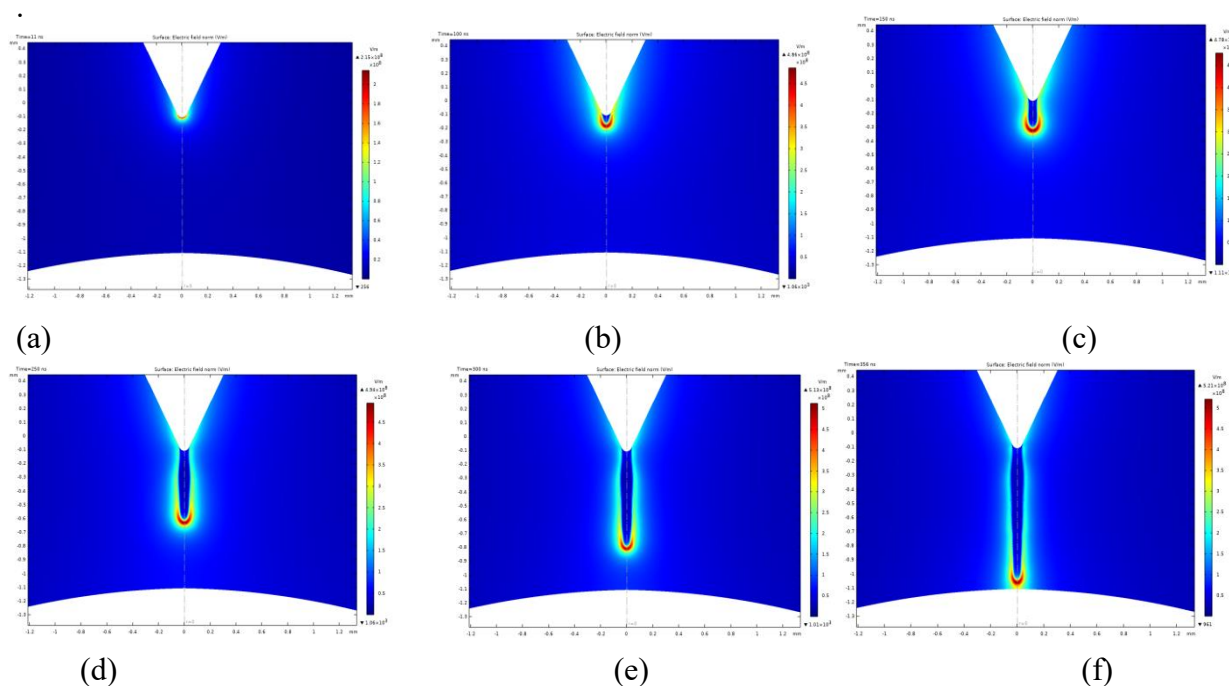


**Figure 3:** Streamer discharge evolution from initiation to breakdown stages at different periods (a)11ns (b)100ns (c)150ns (d)250ns (e)300ns (f)356ns



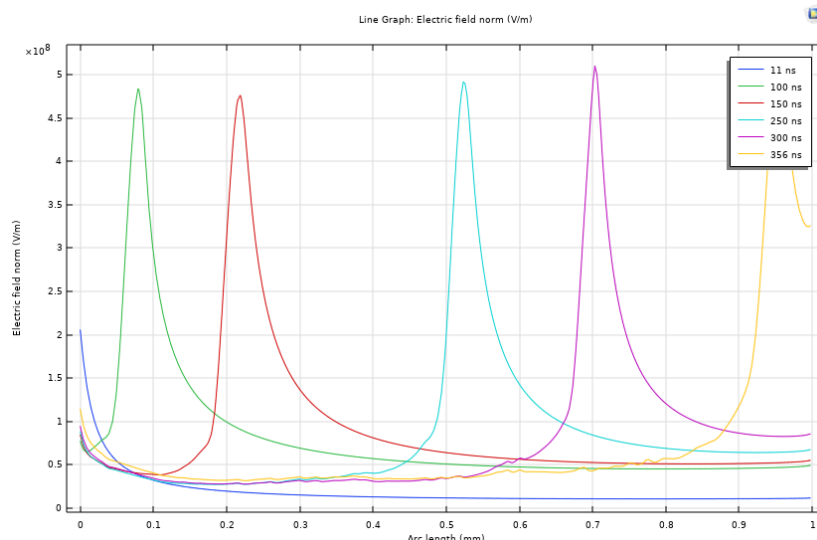


**Figure 4:** A line graph for the electric field distribution along the axis of streamer discharge at different periods from initiation at 11ns to breakdown at 356 ns.

The three stages of a streamer discharge breakdown process are start, propagation, and breakdown. The location of the streamer discharge head determines which stage it is in. During the initial(start) stage, Figure 3a, the needle electrode is the source of the streamer discharge. It begins as a localized ionization region and gradually develops into a propagating streamer. The propagation stage, Figure 3b, c, d, e, is challenging to simulate because it requires significant computational capabilities. At this point, the streamer discharge spreads and moves across the dielectric medium. The surrounding medium is gradually ionized and breaks down along the streamer's journey. The breakdown stage occurs when the streamer discharge touches the sphere electrode (Figure 3e). The breakdown process is currently considered to be complete. Electrical current can flow between the needle and the sphere electrodes because the streamer discharge makes a conductive route.

In the first stage, as streamers leak into the oil, the electric field strength at the streamer front gradually increases. At the beginning of the streamer discharge, the electric field is relatively small but progressively intensifies. An accumulation of ionization occurs at the streamer front as a result of the electric field's increased gradient. Consequently, the streamer velocity during this stage is relatively slow due to the increasing electric field strength. As time progresses, the streamer velocity accelerates more rapidly due to the influence of electrostatic forces on the charged particles. The streamer's length at any given time can be used to calculate their speed. The time evolution of the electric field, the streamer diameter, and the streamer velocity are displayed in Table 1.

**Table 1 :** Streamer characteristics

Periods (ns)	The electric field at the streamer front (V/m)	Streamer velocity km/s	Streamer diameter (mm)
11	$2.15 \times 10^8$	0.36	0.0556
100	$4.86 \times 10^8$	1.27	0.182
150	$4.78 \times 10^8$	1.827	0.202
250	$4.94 \times 10^8$	2.294	0.198
300	$5.13 \times 10^8$	2.482	0.174
356	$5.21 \times 10^8$	2.780	0.168
The average on all periods	$5.18 \times 10^8$	1.835	0.163

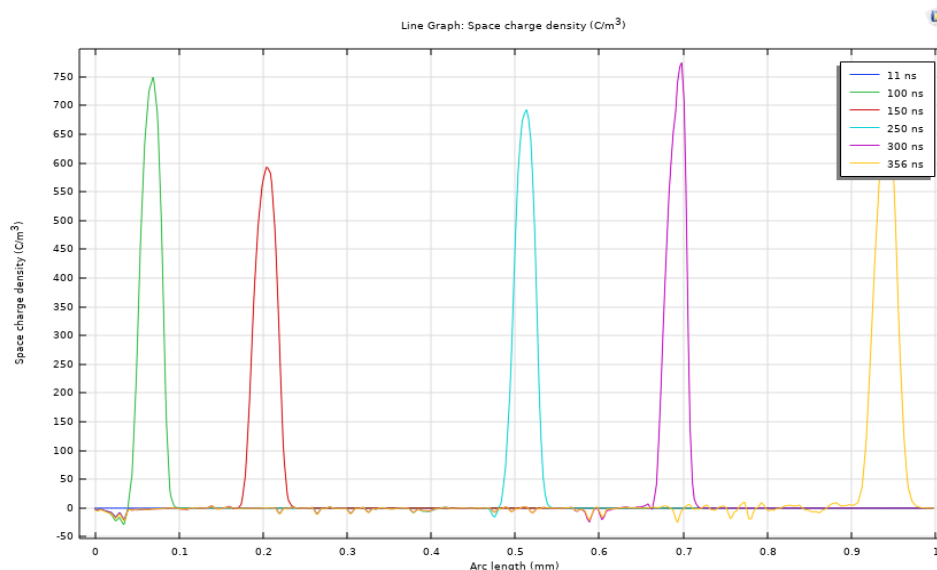


It was indicated that the minimum value observed in the streamer velocity during the initiation stage was 0.36 km/s at 11 ns, while the maximum value was 2.78 km/s at 356 ns. Also, as in Table 1, the streamer diameter started at 0.0556 mm and developed with time to 0.168 mm.

At the propagation stage, the velocity of charged carriers and the ionization process in front of the streamer front are in balance. Moreover, there is equilibrium in the distortion of the electric field brought forth by the space charge area. As a result, the shape of the streamer discharge remains unaltered, only expanding along the z-axis. The velocity of the streamer during the propagation stage remains relatively constant. The recorded velocities are consistent in behavior with the results obtained from a numerical analysis mentioned by Hwang et al. [24]. Additionally, as the streamer discharge progresses, the strength of the electrical field varies and holds steady at various intervals; the stability of the streamer and electric field propagation contribute to the strength of the electric field. The ionization of molecules and the transport of charged carriers in the presence of a strong electric field impact these highly interconnected processes. At the leading edge of the streamer discharge, the amplitude of this electric field closely resembles the findings from the experimental investigation of Lesaint and Top [25].

The electric field rapidly redistributes at 356 ns the moment the streamer discharge contacts the sphere electrode (the cathode). Numerous electrons and ions are produced close to the cathode as a result of this redistribution. Consequently, the streamer's stability and form alter. These changes signal that the streamer discharge has come to the breakdown point, bringing the breakdown phase to an end, upon hitting the ground sphere electrode.

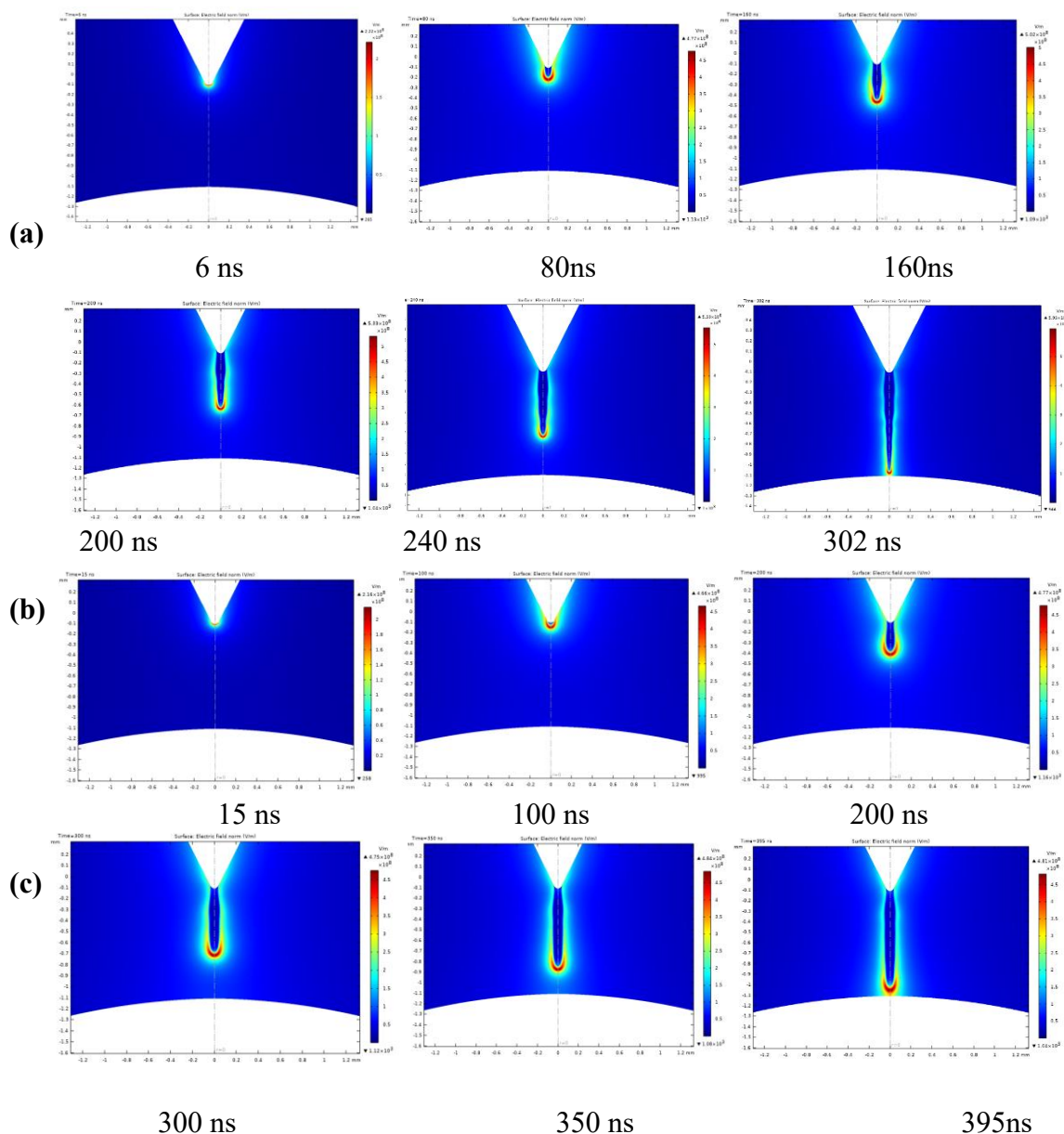
Figure 5 shows the morphology and process of the space charge density. Streamers, or plasma channels, are visible, flowing at different moments from the needle electrode to the sphere electrode. In the oil model system, the density of space charge distribution is positioned above the electric field characteristics. Despite this, Figure 4 (a, b, c, d, e, f) shows a high correlation between the density of space charge distribution and the peaks in the electric field profile. The space charge distribution over time shows that mostly positive ions enhance the electric field dispersion. Positive ions are produced by the electric field-dependent molecular ionization process. High-mobility electrons are swept out of the ionization zone and taken up by the positive electrode, as explained by Hwang et al. [30].



**Figure 5:** A line graph for the space charge distribution along the axis of streamer discharge at different times from initiation at 11 ns to breakdown at 356 ns.

### 3.2. Effect of Rising Time

The rising time of the applied voltage impulse is an important parameter affecting the discharge behavior between the two electrodes. To examine this effect, the same procedure was repeated at different rising times (25, 50, 75, and 100 ns); the streamer was tracked from initiation to breakdown, and the characteristics are shown in Table 2. Figure 6 illustrates a surface distribution for the time development of the electric field (according to streamer development) at different rise times from the streamer discharge initiation at the tip of the needle electrode to its breakdown at the spherical electrode.



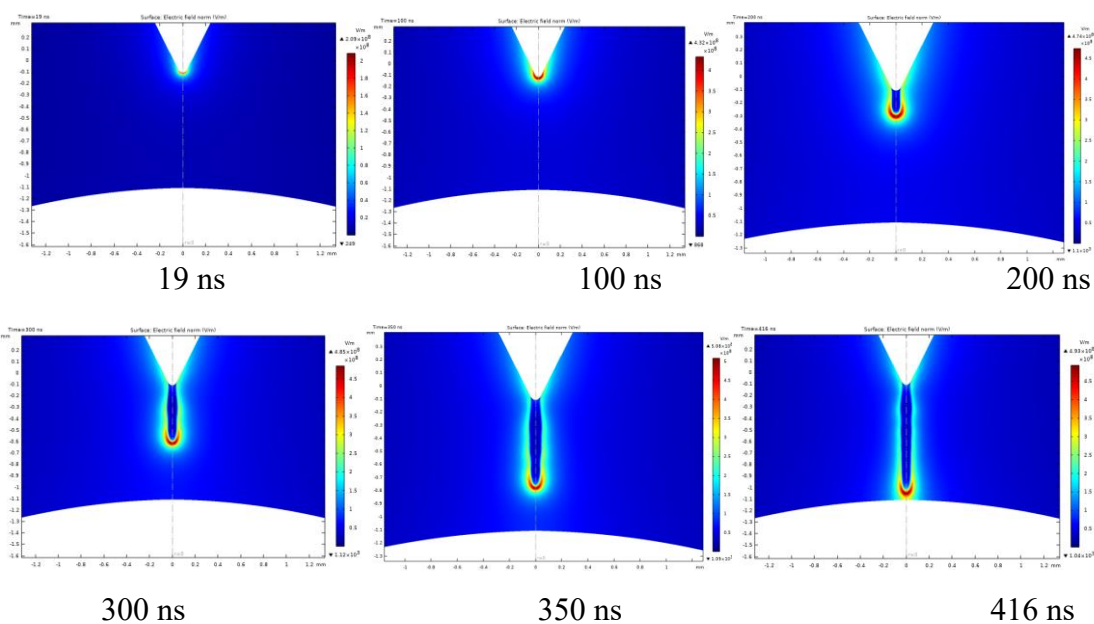


**Figure (6):** Streamer discharge evolution with applied voltage impulse rising times a) 25 ns, b) 75 ns, and c) 100 ns.

As shown in Figure 6, for all values of rising times, the streamer generally depicted the same behavior as described in Figure 5. However, a more detailed analysis shows that the rising time affects the characteristics of the streamer, as summarised in Table 2.

**Table 2:** Streamer characteristics for different rising times

Rising time (ns)	Periods (ns)	Initiation time (ns)	The electric field at the streamer front (V/m)	Streamer velocity (km/s)	Streamer diameter (mm)	Breakdown voltage (kV)
25	6	6	$2.22 \times 10^8$	1.15	0.192	79
	80		$4.77 \times 10^8$	2.058	0.219	
	160		$5.02 \times 10^8$	2.45	0.212	
	200		$5.33 \times 10^8$	2.49	0.184	
	240		$5.53 \times 10^8$	2.77	0.142	
	302		$5.95 \times 10^8$	3.2	0.1036	
	The average on all periods		$4.80 \times 10^8$	2.353	0.175	
50	11	11	$2.15 \times 10^8$	0.36	0.0556	85
	100		$4.36 \times 10^8$	1.27	0.182	
	150		$4.78 \times 10^8$	1.827	0.202	
	250		$4.94 \times 10^8$	2.294	0.198	
	300		$5.13 \times 10^8$	2.482	0.174	
	356		$5.21 \times 10^8$	2.780	0.168	
	The average on all periods		$4.42 \times 10^8$	1.835	0.163	
75	15	14	$2.16 \times 10^8$	0.058	0.024	96
	100		$4.66 \times 10^8$	0.935	0.196	
	200		$4.77 \times 10^8$	1.816	0.2	
	300		$4.75 \times 10^8$	2.331	0.204	
	350		$4.84 \times 10^8$	2.53	0.19	
	395		$4.81 \times 10^8$	2.622	0.208	
	The average on all periods		$4.331 \times 10^8$	1.715	0.170	
100	19	19	$2.09 \times 10^8$	0.37	0.024	100
	100		$4.32 \times 10^8$	0.69	0.187	
	200		$4.74 \times 10^8$	1.276	0.197	
	300		$4.85 \times 10^8$	1.81	0.202	
	350		$5.08 \times 10^8$	2.007	0.198	
	416		$4.93 \times 10^8$	2.376	0.196	
	The average on all periods		$4.335 \times 10^8$	1.421	0.167	

Table 2 shows that even as the electric field at the streamer front and streamer velocity drops, the initiation time rises as the rising time increases. Additionally, there are some variations in the diameter of the streamers at the stable point. The delay in the applied voltage rising can be used to explain the decrease in the electric field, and the same delay can be used to explain the increase in start time and the decrease in streamer velocity. All this clarifies why the breakdown voltage rises as the rising time increases. Stated differently, a quicker rise time results in an increase in the streamer discharge diameter because an electric shock shocks the liquid molecules, particularly those close to the tip electrode. The charge distribution widens to form a larger area surrounding the tip electrode as a result of a faster-rising electric field limiting the electrons' ability to disperse across the liquid volume. Consequently, this leads to a larger streamer discharge diameter [29]. Also, streamers generated by steeper applied voltages demonstrate a slightly reduced maximum electric field at the streamer head compared to streamers produced by voltages with shorter rise times. The larger curvature radii of the streamer heads formed by shorter rise times are primarily attributed to this decline in electric field intensity. Streamer velocity decreases instantaneously as a result of these dips in the highest electric field ahead of the streamer and the required breakdown voltage must be greater.

#### 4. Conclusion

The process of initiating and propagating streamer discharge in transformer oil was examined in this research utilizing the COMSOL Multiphysics package version 6.0 and the numerical finite element method. The findings gathered allow for the following conclusions to be made: The electric field was less due to the applied voltage impulse's delayed rising time, which in turn delayed the streamer's initiation at the needle electrode. The decrease of the electric field resulted in a decrease in the streamer's velocity, which in turn led to a higher voltage that broke the insulating liquid gap between the two electrodes.

#### 5. ACKNOWLEDGMENTS

I finished this study with assistance from the Physics Department at the University of Baghdad.

#### References

- [1] R.P. Joshi, J.F. Kolb, S. Xiao, and K. H. Schoenbach, "Aspects of plasma in water: streamer physics and applications," *Plasma Process and Polymers*, vol.6, no.11 pp.763-777,2009.
- [2] J. Velasco, R. Frascella, R. Albarracín, J. C. Burgos, M. Dong, M. Ren, and L. Yang, "Comparison of positive streamers in liquid dielectrics with and without nanoparticles simulated with finite-element software," *Energies*, vol. 11, no.2, pp. 361,2018.
- [3] F. M. O'Sullivan, " A model for the initiation and propagation of electrical streamers in transformer oil and transformer oil-based nanofluids," Ph.D. dissertation, Department of Electrical Engineering and Computer Science, Massachusetts Institute of Technology, 2007.
- [4] J.-W. G. Hwang, "Elucidating the Mechanisms Behind Pre-Breakdown Phenomena in Transformer Oil Systems," Ph.D. dissertation, Department of Electrical Engineering and Computer Science, Massachusetts Institute of Technology, Cambridge, MA, USA, 2010.
- [5] J.C. Devins, J.R. Stefan, and R.J. Schwabe, "Breakdown and prebreakdown phenomena in liquids," *Journal of Applied Physics*, vol.52, no.7, pp. 4531-4545, 1981.
- [6] Yuan Li; Hai-Bao Mu; Yan-Hui Wei; Guan-Jun Zhang; Shu-Hong Wang; Wei-Zheng Zhang; Zhi-Min Li; Jouya Jadidian, Markus Zahn, " Sub-microsecond streamer breakdown in transformer oil-filled short gaps," *IEEE Transactions on Dielectrics and Electrical Insulation*, vol. 21, no. 4, pp. 1616-1626, 2014.
- [7] R. A. Smith, and R. D. Hill, "Lightning: Physics and Effects," Cambridge University Press, 2008.

- [8] H. Akiyama, "Streamer Discharges in Liquids and their Applications," *IEEE Transactions on dielectrics and electrical Insulation*, vol. 7, no. 5, pp. 646-653, 2000.
- [9] O. Lesaint, A. Saker, P. Gournay, R. Tobazeon, J. Aubin, and M. Mailhot, "Streamer Propagation and Breakdown under AC Voltage in Very Large Oil Gaps," *IEEE Transactions on Dielectrics and Electrical Insulation*, vol. 5, no. 3, pp. 351-359, 1998.
- [10] D. Linhjell, L. Lundgaard, and G. Berg, "Streamer Propagation under Impulse Voltage in Long Point-Plane Oil Gaps," *IEEE Transactions on Dielectrics and Electrical Insulation*, vol. 1, no. 3, pp. 447-458, 1994.
- [11] J. Salazar, N. Bonifaci, A. Denat, and O. Lesaint, "Characterization and Spectroscopic Study of Positive Streamers in Water," in *IEEE International Conference on Dielectric Liquids*, USA, pp. 91-4, 2005.
- [12] J. Jadidian, "Charge Transport and Breakdown Physics in Liquid/Solid Insulation Systems," Ph.D. dissertation, Department of Electrical Engineering and Computer Science, Massachusetts Institute of Technology, Cambridge, MA, USA, 2013.
- [13] R. Morrow and N. Sato, "The discharge current induced by the motion of charged particles in time-dependent electric fields; Sato's equation extended," *Journal Physics D: Applied Physics*, vol. 32, no. 5, L20, 1999.
- [14] High-Voltage Test Techniques- Part 1: General Definitions and Test Requirements, *IEC Standard*, pp. 60060-1, 2010.
- [15] H. S. Smalø, Ø. Hestad, S. Ingebrigtsen, and P. O. Åstrand, "Field dependence on the molecular ionization potential and excitation energies compared to conductivity models for insulation materials at high electric fields," *Journal Applied Physics*, vol. 109, no. 7, pp. 073306, 2011.
- [16] J. Jadidian, M. Zahn, N. Lavesson, O. Widlund, and K. Borg, "Effects of impulse voltage polarity, peak amplitude, and rise time on streamers initiated from a needle electrode in transformer oil," *IEEE Transactions on Plasma Science*, vol. 40, no. 3, pp. 909-918., 2012.
- [17] A. K. Bard and Q. A. Abbas, "Influence of Cylindrical Electrode Configuration on Plasma Parameters in a Sputtering System.," *Iraqi Journal of Science*, vol. 63, no. 8, pp. 3412-3423, 2022.
- [18] R. S. Mohammed, K. A. Aadim, and K. A. Ahmed, "Spectroscopy Diagnostic of Laser Intensity Effect on Zn Plasma Parameters Generated by Nd: YAG Laser," *Iraqi Journal of Science*, vol. 63, no. 9, pp. 3711-3718, 2022.
- [19] Methods for the Determination of the Lightning Impulse Breakdown Voltage of Insulating Liquids, IEC 60897, Switzerland, 1987.
- [20] O. Schenk and K. Gärtner, " Solving unsymmetric sparse systems of linear equations with PARADISO," *Future Generation Computer System*, vol. 20, no. 3, pp. 475-487, 2004.
- [21] Beroual A, Zahn M, Badent A, Kist K, Schwabe A, Yamashita H, Yamazawa K, Danikas M, Chadband W, and Torshin Y, "Propagation and structure of streamers in liquid dielectrics," *IEEE Electrical Insulation Magazine*, vol. 14, no. 2, pp. 6-17, 1998.
- [22] A. Luque, U. Ebert, C. Montijn, and W. Hundsdorfer, "Photoionization in negative streamers: Fast computations and two propagation modes," *Applied physics letters*, vol. 90, no. 8, p. 081501, 2007.
- [23] P. Rodin, U. Ebert, W. Hundsdorfer, and I. Grekhov, "Tunneling-assisted impact ionization fronts in semiconductors," *Journal of applied physics*, vol. 92, no. 2, pp. 958-964, 2002.
- [24] J. G. Hwang, M. Zahn, and L. A. Pettersson, "Mechanisms behind positive streamers and their distinct propagation modes in transformer oil," *IEEE Transactions on Dielectrics and Electrical Insulation*, vol. 19, no. 1, pp. 162-174, 2012.
- [25] O. Lesaint and T. Top, "Streamer Initiation in Mineral Oil. Part I: Electrode Surface Effect under Impulse Voltage," *IEEE Transactions on Dielectrics and Electrical Insulation*, vol. 9, no. 1, pp. 84-91, 2002.
- [26] L. Lundgaard, D. Linhjell, G. Berg, and S. Sigmond, " Propagation of positive and negative streamers in oil with and without pressboard interfaces," *IEEE Transactions on Dielectrics and Electrical Insulation*, vol. 5, pp. 388-395, 1998.
- [27] O. Lesaint and G. Massala, " Positive streamer propagation in large oil gaps: experimental characterization of propagation modes," *IEEE Transactions on Dielectrics and Electrical Insulation*, vol. 5, pp. 360-370, 1998.

- [28] J. Jadidian, M. Zahn, N. Lavesson, O. Widlund, and K. Borg, "Impulse breakdown delay in liquid dielectrics," *Applied Physics Letters*, vol. 100, no. 19, p. 192910, 2012.
- [29] Dianchun Z, Zhengwei W, Chuntian C, and Weiguo Y, " Discharge characteristics of streamer in liquid dielectric under lightning impulse voltage," *IEEE Annual Report Conference on Electrical Insulation and Dielectric Phenomena*, pp 971-4, 2013.
- [30] J. G. Hwang, M. Zahn, F. M. O'Sullivan, L. A. Pettersson, O. Hjortstam, and R. Liu, "Effects of nanoparticle charging on streamer development in transformer oil-based nanofluids," *Journal of applied physics*, vol. 107, no. 1, p. 014310, 2010.